Amplitude death of identical oscillators in networks with direct coupling

Lucas Illing*
Physics Department, Reed College, Portland, Oregon 97202, USA
(Received 6 April 2016; published 25 August 2016)

It is known that amplitude death can occur in networks of coupled identical oscillators if they interact via diffusive time-delayed coupling links. Here we consider networks of oscillators that interact via direct time-delayed coupling links. It is shown analytically that amplitude death is impossible for directly coupled Stuart-Landau oscillators, in contradistinction to the case of diffusive coupling. We demonstrate that amplitude death in the strict sense does become possible in directly coupled networks if the node dynamics is governed by second-order delay differential equations. Finally, we analyze in detail directly coupled nodes whose dynamics are described by first-order delay differential equations and find that, while amplitude death in the strict sense is impossible, other interesting oscillation quenching scenarios exist.

DOI: 10.1103/PhysRevE.94.022215

I. INTRODUCTION

Coupled oscillators are an effective model for many processes in nature, with examples that include chemical reactions [1], photonics systems [2,3], neurons [4], and many biological processes [5,6]. Such complex systems exhibit a variety of interesting emergent dynamical phenomena induced by the presence of coupling, including several forms of fully and partial synchronized oscillations [7–9] as well as the phenomenon of oscillation quenching [10,11]. The suppression of oscillations through coupling has relevance as a control mechanism, for example, for the stabilization of coupled lasers [3,12] or treatment of neurological disorders [13].

There are two main types of oscillation quenching known in the literature [14,15]: oscillation death and amplitude death. Regarding the terminology, it has been proposed [15] to refer to oscillation death if oscillations are quenched to an inhomogeneous steady state, whereas phenomena that result in the stabilization of a homogeneous steady state should be called amplitude death.

As is true in general, the phenomenon of oscillation quenching may depend on properties of the nonlinear functions governing the node dynamics, properties of the coupling functions, as well as the network topology, coupling weights, and coupling delay times. For example, it is known that amplitude death of two coupled Stuart-Landau oscillators may be caused by mismatches between the frequencies of the oscillators [10,11], coupling through dissimilar variables [16], or time delay in the coupling [17].

Whereas oscillation quenching in networks of identical oscillators with diffusive and delayed coupling has received a lot of attention [14–22], far less is known about directly coupled networks. The purpose of this paper is to fill this gap.

We refer to diffusive coupling if coupling functions have the form $\mathbf{h}(\mathbf{x}_\ell - \mathbf{x}_j)$, where the input to oscillator j from oscillator ℓ depends on the difference of their states (potentially with a relative time shift). Linear diffusive coupling, where $\mathbf{h}$ is a linear function, captures a large class of interaction processes, such as diffusion of chemicals due to a concentration difference or ohmic current due to a difference of electric potentials. A second important form of interaction is direct coupling, referring to coupling functions $\mathbf{h}(\mathbf{x}_\ell)$ that are entirely independent of the state $\mathbf{x}_j$ of the receiving oscillator. An example of systems with such coupling are optoelectronic oscillators, where links are established by adding optical power emitted by system ℓ to the receiver j [8,23–29]. As already pointed out in the pioneering paper on amplitude death by Aronson *et al.* [10], the dynamical behavior of directly coupled oscillators may substantially differ from diffusively coupled ones.

Motivating the current study is the fact that amplitude death is possible in networks of weakly coupled identical oscillators close to an Andronov-Hopf bifurcation if they interact via linear diffusive coupling links with time delay [17,30], but amplitude death is impossible for such networks if the oscillators interact via direct coupling [30]. Crucial to this result is the assumption of weak coupling, which permits the use of normal form theory. In contradistinction to this previous work, we investigate in the current paper networks with arbitrary coupling strengths. We focus on directly coupled networks of identical oscillators and consider amplitude death arising in systems where both the node dynamics and the coupling may include time delay.

For the purpose of this paper we say that *amplitude death in the strict sense* occurs if the homogeneous steady state that is stabilized through coupling does exist in the absence of coupling and if the uncoupled systems are close to the Andronov-Hopf bifurcation that destabilized the steady state.

In general, we find that amplitude death in the strict sense is far less likely in networks of identical oscillators with direct coupling as compared to diffusively coupled networks. Intuitively, this can be explained by the fact that in diffusively coupled networks the dependence of the coupling function on the state of the receiver $\mathbf{x}_j$ can introduce an additional dissipative term for the right choice of coupling function and network topology. This term, which tends to stabilize the steady state, is entirely missing in the case of direct coupling.

A second effect that plays a role is that only links connecting distinct nodes are permitted. Coupling topologies that have coupling links from a node to itself do not belong to the class of directly coupled networks. It is well known that such self-feedback has a stabilizing effect not only for network steady states but also for chaos synchronization [27]. Mathematically, the absence of such self-feedback network links implies that

*illing@reed.edu

the coupling matrix has zero trace and, therefore, the sum of network eigenvalues is zero. We make use of this restriction to demonstrate the impossibility of amplitude death for certain classes of node dynamics.

The paper is organized as follows: We show that amplitude death in directly coupled networks is impossible if coupling delays are large (Sec. II) or if the nodes are Stuart-Landau oscillators (Sec. III). In Sec. IV, directly coupled networks of first-order delay differential equations (DDEs) are discussed in detail because they represents an interesting case of intermediate-complexity node dynamics, one where amplitude death in the strict sense is impossible but other oscillation quenching scenarios are present. Finally, we provide an example in Sec. V that demonstrates the existence of amplitude death in the strict sense for systems of directly coupled second-order DDEs. The results are summarized in Sec. VI.

II. LARGE COUPLING DELAYS

In this section, we show that the zero steady state of directly coupled networks of identical oscillatory systems cannot be stabilized if the coupling delays are large. Therefore, amplitude death is impossible. This holds for any network topology, link weights, or chosen coupling delay times.

Consider a network of N identical delay-coupled delay oscillators ($\mathbf{x}_j \in \mathbb{R}^d, j = 1,\ldots,N$):

$$\dot{\mathbf{x}}_j(t) = \mathbf{f}[\mathbf{x}_j(t),\mathbf{x}_j(t-1)] + \sum_{\ell\neq j} g_{j\ell}\,\mathbf{h}[\mathbf{x}_\ell(t-\tau_{j\ell})]. \quad (1)$$

Here, $\mathbf{f}$ is a (nonlinear) function describing the dynamics of an isolated unit and time has been rescaled, without loss of generality, such that the units' internal self-feedback delay is equal to 1. The $g_{j\ell}$ are elements of the real-valued coupling matrix that determines the topology and the strength of each link in the network, $\tau_{j\ell}$ are the coupling delays, and $\mathbf{h}$ is a possibly nonlinear coupling function. The coupling is *direct* in the sense that the input function $\mathbf{h}$ to node j is independent of the state $\mathbf{x}_j$ of the jth node. It is assumed, without loss of generality, that $\mathbf{f}(0,0) = 0$, such that zero is a steady-state solution of the uncoupled system. In addition, we assume that $\mathbf{h}(0) = 0$, such that the contribution from the coupling terms is zero at the homogeneous network steady-state solution $\mathbf{X} = 0$, where $\mathbf{X}$ is a $(d\cdot N)$ column vector, $\mathbf{X} = (\mathbf{x}_1,\mathbf{x}_2,\ldots,\mathbf{x}_N)^T$. That is, the coupling is noninvasive and the network homogeneous steady state exists for any choice of coupling weights $g_{j\ell}$. Thus, the $\mathbf{h}(0) = 0$ assumption allows us to consider arbitrary network topologies. We further assume that the steady state $\mathbf{x}_j = 0$ of a single uncoupled system is unstable.

To determine the steady-state stability of the network, we linearize Eq. (1):

$$\dot{\mathbf{X}}(t) = [\mathbf{I}_N \otimes \mathbf{A}]\,\mathbf{X}(t) + [\mathbf{I}_N \otimes \mathbf{B}]\,\mathbf{X}(t-1) + \sum_j \sum_{\ell\neq j} g_{j\ell}[\boldsymbol{\delta}_{j\ell} \otimes \mathbf{C}]\,\mathbf{X}(t-\tau_{j\ell}). \quad (2)$$

Here $\otimes$ is the Kronecker product, $\mathbf{I}_N$ the N-dimensional identity matrix, $\mathbf{A} = D_x\mathbf{f}(0,0)$ the $d\times d$ Jacobian matrix of derivatives of $\mathbf{f}$ with respect to the first (nondelayed) argument calculated at the steady state, $\mathbf{B} = D_y\mathbf{f}(0,0)$ the Jacobian derivative with respect to the second (delayed) argument, $\mathbf{C} = D\mathbf{h}(0)$ the $d\times d$ Jacobian matrix of the coupling function, and $\boldsymbol{\delta}_{j\ell}$ an $N\times N$ matrix with element $j\ell$ equal to 1 and all other entries zero.

The stability of the steady state is determined by the complex-valued spectrum of eigenvalues Λ that are the roots of the characteristic equation

$$\det([\mathbf{I}_N \otimes \mathbf{I}_d]\,\Lambda - [\mathbf{I}_N \otimes \mathbf{A}] - [\mathbf{I}_N \otimes \mathbf{B}]\,e^{-\Lambda} - \sum_j \sum_{\ell\neq j} g_{j\ell}[\boldsymbol{\delta}_{j\ell} \otimes \mathbf{C}]\,e^{-\Lambda\,\tau_{j\ell}}) = 0. \quad (3)$$

The spectrum Λ of a linear DDEs with large delay splits into two different parts: the so-called pseudocontinuous spectrum and strong spectrum [31]. Eigenvalues Λ_+ belonging to the strong unstable spectrum have the property that they do not scale with the coupling delay and have a positive real part [31]. Considering such eigenvalues in the $\tau_{j\ell}\to\infty$ limit, one finds that Eq. (3) reduces to

$$\det(\Lambda_+\,\mathbf{I}_d - \mathbf{A} - \mathbf{B}\,e^{-\Lambda_+}) = 0. \quad (4)$$

Solutions Λ_+ to this equation exist by assumption, because Eq. (4) corresponds the characteristic equation of a single uncoupled system, which has an unstable zero steady state. This shows that the unstable spectrum of the single uncoupled systems persists if the systems are joined into a network by direct coupling links with large coupling delays. The zero steady state remains unstable for any network topology and choice of coupling weights.

This shows that amplitude death in the strict sense is impossible not only in the limit of weak coupling strengths [30] but also in the limit of large coupling delays if network links implement direct coupling. Therefore, we explore next whether amplitude death can occur in directly coupled networks if arbitrary values for the coupling strengths and coupling delays are permitted. To do so, we make, in the following, the simplifying assumption that the coupling delays are matched, i.e., $\tau_{j\ell} = \tau$ in Eq. (1). We also need assumptions about the node dynamics. First, in Sec. III, it is assumed that the nodes have no internal delay and that the node dynamics close to the zero steady state are of focus type. Then, in Sec. IV, nodes with internal delay are considered but it is assumed that the nodes' evolution is captured by first-order delay differential equations.

III. ORDINARY DIFFERENTIAL EQUATIONS WITH UNSTABLE FOCUS

A necessary ingredient for the appearance of amplitude death is that an unstable steady state of the uncoupled systems becomes locally stable due to coupling. Linear stability analysis suffices to determine whether this condition is satisfied. Such analysis shows that identical Stuart-Landau oscillators exhibit the phenomenon of amplitude death if they interact via identical time-delayed diffusive coupling links [17]. Here we show that no such stabilization is possible for the case of time-delayed direct coupling.

Consider a N-node network, where each node is a dynamical system modeled by an ordinary differential equation (ODE) with an unstable steady state of focus type at the origin. The edges are direct coupling links of weight $g_{j\ell}$ ($g_{j\ell}\in\mathbb{R}$). The

coupling delay is assumed to be τ for all edges. We presume that the relevant local dynamics takes place on an attractive manifold describable in terms of a complex variable z. The linearized equation for the jth system is taken to be

$$\dot{z}_j(t) = (a + i\,\omega_0)\,z_j(t) + r\,e^{i\phi_0}\sum_{\ell\neq j}^{N} g_{j\ell}\,z_j(t-\tau). \quad (5)$$

Here $a + i\,\omega_0$ is the eigenvalue of the focus of the uncoupled systems. The steady state is unstable if $a > 0$. The coupling phase ϕ_0 and magnitude r ($r \in \mathbb{R}^+$) arise from the linearization of the coupling function. It is important to note that we do not assume weak coupling. Therefore, to arrive at Eq. (5) as a reduced model of the full systems, certain restrictive assumptions regarding the coupling function have to be made, including the assumption that inputs to node j act on the locally unstable directions modeled by z_j and that the coupling preserves rotational symmetry. This means, for example, that coupling functions that act on the real part of z_j only [32] are excluded from the discussion. Nevertheless, Eq. (5) covers a wide range of possible ODEs. In particular, networks of Stuart-Landau oscillators with delayed direct coupling are included, allowing comparison to the known results for diffusive coupling [17].

The simplifying assumption of identical coupling delays τ is essential to the analysis because it allows us to use the master stability function (MSF) approach [33]. However, we note that for a network of just two oscillators the assumption of identical coupling delays is not a restriction because a simple coordinate transformation [34] maps the unequal coupling delay case to the one with identical delays.

If the $N \times N$ coupling matrix with elements $g_{j\ell}$ is diagonalizable, then the stability of the steady state is governed by the eigenvalues γ_k of the coupling matrix and the MSF. For steady states, the MSF is defined as the maximum real part of the spectrum Λ as a function of the complex argument κ. Introducing the notation $\Lambda = \Lambda' + i\Lambda''$ for the real and imaginary part of Λ, we may denote the MSF by $\Lambda'_{\max}(\kappa)$. The spectrum Λ arises as the solution of the characteristic equation

$$\Lambda = (a + i\,\omega_0) + \kappa\,r\,e^{i\phi_0}\,e^{-\Lambda\,\tau}. \quad (6)$$

The steady state is stable for a given coupling topology if the MSF is negative at all network eigenvalues γ_k of the coupling matrix, that is, if $\Lambda'_{\max}(\gamma_k) < 0$.

The MSF can be found analytically from Eq. (6), as shown in Appendix A. The result is displayed in Fig. 1, where the region of stable steady states is displayed in 3D parameter space. The three relevant effective parameters are the scaled stability parameter of the focus, $a\,\tau$, together with the real and imaginary part of ζ, where $\zeta = \kappa\,\tau\,r\exp[i(\phi_0 - \omega_0\tau)]$ is proportional to the complex argument κ of the MSF rotated through an angle $\phi_0 - \omega_0\tau$. In other words, the MSF of any system described by Eq. (5) is a scaled and rotated version of the MSF shown in Fig. 1, depending on the values of ϕ_0, ω_0, τ, and r. As seen in Fig. 1(a) and Fig. 1(c) and as shown in Appendix A, the MSF has no negative region if $a\,\tau > 1$. Although the MSF for $a\,\tau = 0.5$ has a negative region, it lies entirely in the left complex half plane, as shown in Fig. 1(b). No network with direct coupling links can have all its network eigenvalues γ_k in this region because the coupling

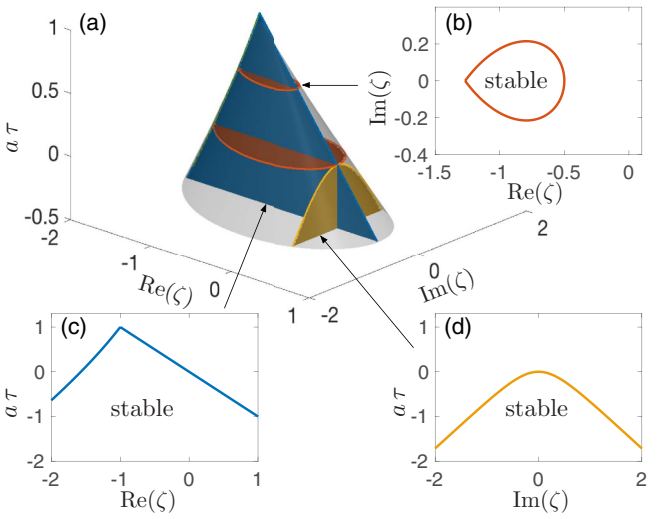

FIG. 1. Steady-state stability region: (a) $\Lambda'_{\max} < 0$ below gray transparent surface and (b) slice defined by $a\,\tau = 0.5$, corresponding to a rotated and scaled version of the MSF with $\Lambda'_{\max}(\kappa) < 0$ inside (red) boundary (c) $\mathrm{Im}(\zeta) = 0$ slice (d) $\mathrm{Re}(\zeta) = 0$ slice

matrix of networks with direct coupling has zero trace (since $g_{ii} = 0$) and therefore $\sum_k \gamma_k = 0$. The condition $\sum_k \gamma_k = 0$ can be satisfied if the negative region of the MSF starts to extend into the right complex half plane, which happens if $a\,\tau < 0$. This is seen most clearly in Fig. 1(d), which depicts the stability region on the surface defined by $\mathrm{Re}(\zeta) = 0$. This shows that a stable steady state of directly coupled networks is only possible if the uncoupled systems already have a stable focus at the origin ($a < 0$). If the focus is unstable ($a > 0$), then no choice of network topology, coupling weights, or coupling delay τ will stabilize the steady state. This is in stark contrast to diffusively coupled Stuart-Landau oscillators, where delayed coupling gives rise to amplitude death [17].

IV. FIRST-ORDER DELAY DIFFERENTIAL EQUATIONS

The question arises whether increasing the complexity of the dynamics of the identical network nodes allows for the appearance of amplitude death in networks of directly coupled identical systems. DDEs are richer in their possible dynamics than ODEs, due to the fact that they have an infinite dimensional state space, but much simpler than partial differential equations. We therefore analyze in some detail networks of first-order DDEs, the simplest DDE possible, and show that there exist networks for which direct coupling results in a stable zero steady state. However, despite steady-state stabilization, the analysis will demonstrate that amplitude death in the strict sense cannot occur, although other forms of oscillation quenching are possible. One needs to consider directly coupled second-order DDEs to find amplitude death in the strict sense.

A. Linear stability analysis

To simplify the analysis, we again assume that all coupling delays are matched and equal τ. With this, Eq. (2), describing

the linear stability of the steady state, reduces to

$$\dot{\mathbf{X}}(t) = a\,\mathbf{X}(t) + b\,\mathbf{X}(t-1) + \mathbf{G}\,\mathbf{X}(t-\tau), \tag{7}$$

where we have introduced, for clarity of notation, the symbols $a,b\,(\in\mathbb{R})$ instead of $\mathbf{A},\mathbf{B}$, respectively. The $N\times N$ real-valued coupling matrix $\mathbf{G}$ has elements $c\,g_{j\ell}$, where c ($c\in\mathbb{R}$) is the derivative of the coupling function evaluated at the steady state.

Within the MSF approach, the characteristic equation corresponding to Eq. (7) is

$$\Lambda = a + b\,e^{-\Lambda} + \kappa\,e^{-\Lambda\tau}. \tag{8}$$

The stability of the steady state at the origin only depends on the real part of Λ. Complex conjugation of Eq. (8) shows that if the zero steady state is stable for some $\kappa=\kappa'+i\kappa''$, then it is also stable for $\kappa=\kappa'-i\kappa''$. Therefore, the MSF must be symmetric with respect to the κ' axis.

The network eigenvalues γ_k are either real or form complex conjugate pairs. The symmetry of the MSF means that if one of the eigenvalues γ_k of a complex conjugate pair falls within a negative region of the MSF, then the other one does as well. In contrast, while the condition $\sum_k \gamma_k = 0$ means that the existence of eigenvalues with negative real part imply the existence of other eigenvalues with positive real part, no such symmetry exists for the MSF. One therefore obtains the following necessary and sufficient condition for the MSF: Assuming that the MSF forms one connected region in the κ plane (as is the case for all the examples we consider), then there exist networks with direct coupling that have a stable zero steady state if and only if the negative region of the MSF includes an interval of the imaginary axis.

To determine the MSF for given parameters τ, a, and b, we find the boundary curves in the κ plane where one of the roots of the characteristic equation, Eq. (8), crosses the imaginary axis ($\Lambda = i\Omega$). These Ω-parameterized curves are given by

$$\kappa' = -a\,\cos(\Omega\tau) - b\,\cos(\Omega\tau-\Omega) - \Omega\,\sin(\Omega\tau), \tag{9a}$$

$$\kappa'' = -a\,\sin(\Omega\tau) - b\,\sin(\Omega\tau-\Omega) + \Omega\,\cos(\Omega\tau), \tag{9b}$$

and define regions in the κ plane with a constant number of roots Λ_k that have positive real part (see Fig. 2). We refer to this number as the unstable dimension. The unstable dimension increases (decreases) as a boundary is crossed in the direction of increasing κ' if, at the boundary,

$$\mathrm{sgn}\left[\frac{\partial\Lambda'}{\partial\kappa'}\right] = \mathrm{sgn}[\cos(\Omega\tau) + b\,\cos(\Omega\tau-\Omega) + \kappa'\tau] \tag{10}$$

is positive (negative). To determine the region in the κ plane where the unstable dimension is zero, i.e., the stable region, we find the unstable dimension at the origin and then count how many boundary curves are crossed, keeping track of the sign of the change via Eq. (10).

The unstable dimension at the origin is known because at $\kappa=0$ the systems are uncoupled first-order DDEs with real coefficients. Their stability and normal forms are well established [35,36]. The stability problem is also a special case of first-order DDEs with complex coefficients, discussed in Appendix A. That is, it corresponds to Eq. (A1) with $\alpha=a$ and $\beta=b$, which implies $\zeta=b$, with the result shown in Fig. 1(c) and reproduced in Fig. 2(f).

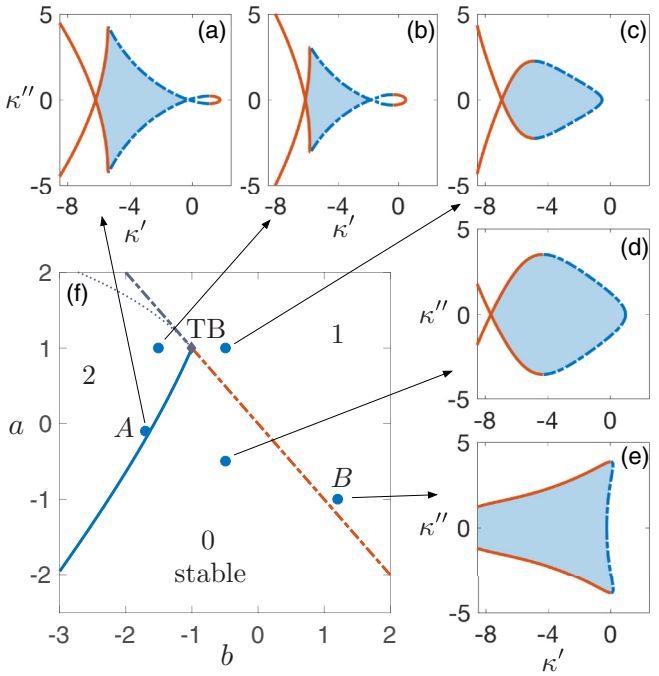

FIG. 2. [(a)–(e)] MSF for $\tau=0.2$ and (b,a) parameters values: (a) $(-1.7,-0.1)$; (b) $(-1.5,1)$; (c) $(-0.5,1)$; (d) $(-0.5,-0.5)$; (e) $(-1,1.2)$. Unstable dimension is zero in blue (dark gray) shaded region. Unstable dimension increases (decreases) by one as the blue dashed (red solid) boundary line is crossed in the positive κ' direction. (f) Stability diagram of uncoupled system with unstable dimension and region of stable steady state indicated; Andronov-Hopf bifurcation, solid line (blue); $\Lambda=0$-bifurcation, dashed line (red and gray); Takens-Bogdanov bifurcation, TB (diamond); and transition from a complex conjugate pair to a pair of (positive) real roots, dotted line (gray).

For any given value of a and b, the region with unstable dimension zero in the κ plane (the MSF) can thus be determined, with τ being the only remaining free parameter. In Figs. 2(a)–2(e), the MSF for various points in the a-b plane is depicted for $\tau=0.2$. It is seen that in each case there exists a stable region, one with an unstable dimension equal zero. However, for stabilization of the steady state via direct coupling to be possible, this region must contain part of the imaginary axis. Only Fig. 2(d) and Fig. 2(e) satisfy this requirement. Of these, the stable region in Fig. 2(d) includes the origin, meaning that the steady state is stable even in the absence of coupling. Thus, only Fig. 2(e) represents a case where direct coupling can lead to a stabilization of the steady state.

The dependence of the MSF on τ is depicted in Fig. 3 for the a,b parameters of point A in Fig. 2(f). It is seen that the region with unstable dimension zero shrinks as τ increases and disappears for sufficiently large τ, in agreement with Sec. II. Furthermore, none of the τ values produces a stable region that contains the imaginary axis, as seen by the magnified depiction of the MSF in Figs. 3(e)–3(g). This suggests that the zero steady state at point A in Fig. 2(f), close to the Andronov-Hopf bifurcation, cannot be stabilized through direct coupling.

We now present evidence showing that stabilization by direct coupling is impossible not only for point A in Fig. 2(f)

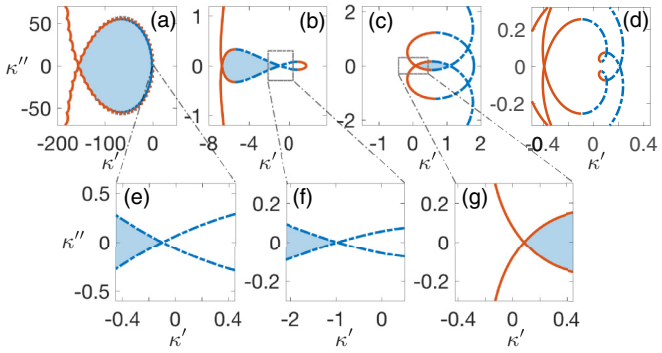

FIG. 3. MSF for $b = -1.7, a = -0.1$, corresponding to A in Fig. 2(f), with τ equal [(a) and (e)] 0.01, [(b) and (f)] 0.33, [(c) and (g)] 1.8, and (d) 20.

but for all a-b parameter values of the node's first-order DDE that are close to the Andronov-Hopf bifurcation.

To do this, we consider optimal networks and compute numerically the volume in $a - b - \tau$ parameter space for which there exist delay-coupled networks of identical first-order DDEs with matched coupling delays τ that stabilize the steady state. One notes that the optimal choice of networks with direct coupling are those with network eigenvalues of zero real part, $\mathrm{Re}(\gamma_k) = 0$, because these networks may become stabilizing as soon as the stable (negative) region of the MSF includes the imaginary axis. Such networks exist. An example are networks with skew-symmetric coupling matrices $\mathbf{G}$, where each connected pair of nodes has one directed inhibitory link and a second corresponding excitatory link in the opposite direction with equal coupling strength, $g_{j\ell} = -g_{\ell j}$. Since the real part κ' of the MSF parameter κ is zero for optimal networks, it suffices to determine numerically, for each $a - b - \tau$ parameter triplet, the minimal value of the MSF as a function of the imaginary part κ''. The result is shown in Fig. 4.

We find that stabilization of the zero steady state via direct coupling is possible for small τ and a considerable range of $a - b$ parameters, all adjacent to the $\Lambda = 0$ bifurcation boundary (see the green region in Fig. 4). In contrast, for $a - b$ parameters close to the Andronov-Hopf bifurcation line, the numerical evidence suggests that zero steady-state stabilization via direct-coupling links is impossible.

In the $\tau \to 0$ limit the boundary can be determined analytically as shown in Appendix B. The result is depicted in Fig. 4(b), where there exist choices of the coupling parameters that stabilize the zero steady state for the a-b parameter region below the red boundary curve. The stable region is divided into two parts: the blue shaded region, in which the uncoupled oscillators would have a stable zero steady state, and the green shaded region, in which coupled networks exist that stabilize the zero steady state.

Another case that is analytically easy to treat is the one where the coupling delay and the internal delay are matched, i.e., $\tau = 1$. In this case the MSF for the optimal choice $\kappa' = 0$ is identical to the one discussed in Appendix A and displayed in Fig. 1 if one makes the replacement $a\tau \to a$, $\mathrm{Re}(\zeta) \to b$ and $\mathrm{Im}(\zeta) \to \kappa''$. It is seen that stabilization of the zero steady state through coupling is impossible for the $\tau = 1$ case because the optimal choice of κ'' is the uncoupled network with $\kappa'' = 0$, whereas all other choices of κ'' lead to smaller or no stability regions in the a-b parameter plane.

The numerical results in Fig. 4 show that the region that can be stabilized through coupling shrinks as τ is increased from zero. The numerics suggest that the $\tau = 0$ and $\tau = 1$ cases are the relevant limiting cases, with $\tau = 0$ corresponding to the maximal a-b region being stabilizable, whereas stabilization becomes impossible for $\tau \geqslant 1$.

B. Amplitude death in the strict sense is impossible

The clearest example of amplitude death is one where the uncoupled systems each have an unstable steady state at the origin surrounded by a stable limit cycle, whereas the coupled oscillators have a stable zero steady state. Typically, the steady-state stabilization takes place due to an inverse Andronov-Hopf bifurcation as the coupling strength is increased. As mentioned

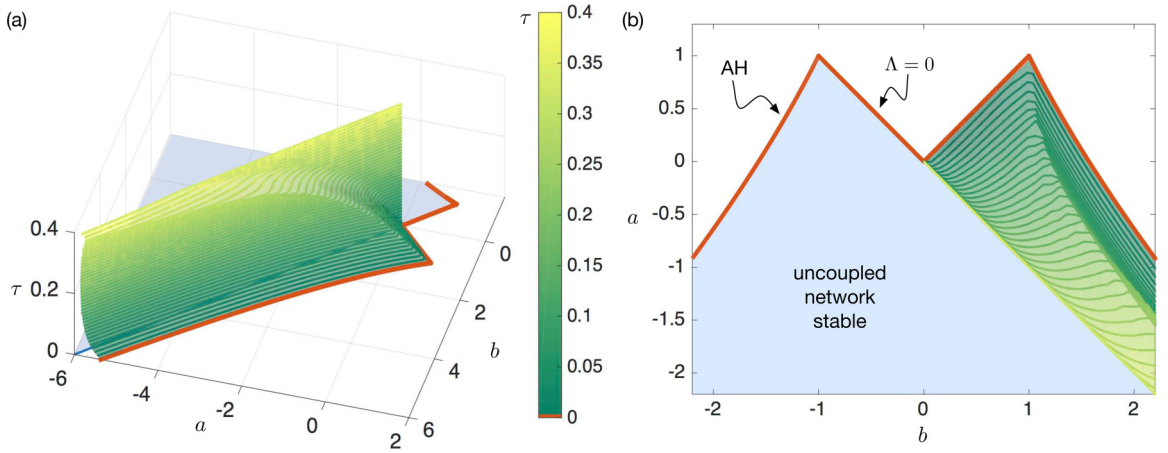

FIG. 4. Stability region for optimal networks. (a) Upper boundary (transparent green) of the a-b-τ parameter region where the zero steady state is stabilized by coupling. Uncoupled networks are stable in the (blue) shaded region (shown here for $\tau = 0$ only, the corresponding volume would extend "upward" to all values of τ). (b) Projection onto a-b plane with the boundary (thick red line) corresponding to $\tau = 0$. AH (Andronov-Hopf) and $\Lambda = 0$ label bifurcations of the uncoupled systems [compare to Fig. 2(f)].

in the Introduction, we refer to such clear-cut situations as amplitude death in the strict sense. The issue with directly coupled first-order DDE network nodes, as described by Eq. (7), is that zero steady-state stabilization is unattainable for a-b values close to the Andronov-Hopf bifurcation. Amplitude death in the strict sense is therefore impossible.

This is in contrast to diffusively coupled networks, where delay-coupled first-order delay differential equations are known to exhibit amplitude death in the strict sense for arbitrary coupling strengths above a threshold value and small but nonzero coupling delays [20].

Although amplitude death in the strict sense is impossible for directly coupled networks, as shown by above linear stability analysis, other oscillation quenching scenarios are a possibility. These scenarios arise through nonlocal phenomena that depend on the particular nonlinearities, network topologies, and coupling weights used. We give two examples. In the first, the condition is dropped that the limit cycle of the uncoupled systems is due to an Andronov-Hopf bifurcation of the zero steady state. In the second, the condition is dropped that it is the zero steady state that is to be stabilized through coupling.

C. Oscillation quenching to the zero steady state

We have shown that stabilization is possible close to the $\Lambda = 0$ bifurcation. For this bifurcation, no local limit cycles surrounding the zero steady state exist in the uncoupled systems, yet nonlocal stable limit cycles are a possibility. As an example, consider the two-oscillator system

$$\dot{x}_1 = a\,x_1(t) + b\,f[x_1(t-1)] + c\,f[x_2(t-\tau)], \qquad (11a)$$

$$\dot{x}_2 = a\,x_2(t) + b\,f[x_2(t-1)] - c\,f[x_1(t-\tau)], \qquad (11b)$$

where a and b parametrize the uncoupled systems, c is the coupling parameter, and the node nonlinearity and coupling function are identical and given by $f[x] = x\,(1+5x^2)/(1+x^6)$, a nonlinearity with saturation for large amplitudes. The dynamics of DDEs with nonlinearities of form f have been studied previously using electronic and optoelectronic time-delay devices [37].

For $a = -1$, the zero steady state of the uncoupled systems ($c = 0$) undergoes a pitchfork bifurcation at $b = 1$, as shown in Fig. 5. As a consequence, the zero steady state is unstable for $b = 1.2$. It coexists with stable limit cycles born in Andronov-Hopf bifurcations of the nonzero steady states. Therefore, the trajectories of the uncoupled systems with $b = 1.2$ will diverge from the zero steady state and approach one of the two limit cycles, as confirmed by direct integration of Eq. (11) [Fig. 5(c)], but will converge to the zero steady state if coupled [Fig. 5(d)].

Although this example exhibits oscillation suppression to a homogeneous steady state, and therefore is a case of amplitude death, the phenomenon differs from amplitude death in the strict sense in that (a) the limit cycles of the uncoupled systems are not local and (b) the stability of the homogeneous steady state of the coupled network is only local. For example, starting the coupled network with initial conditions on the limit cycles of the uncoupled systems will result, asymptotically, in oscillatory solutions.

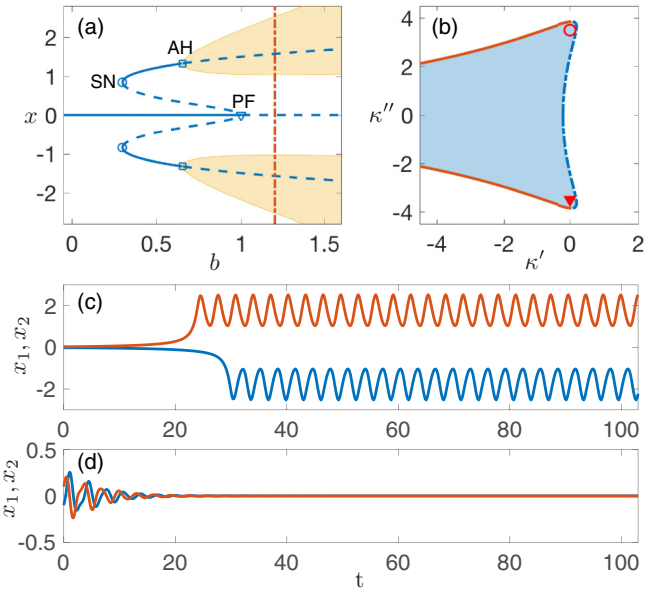

FIG. 5. Oscillation quenching for Eq. (11) with $a - b$ parameters corresponding to point B in Fig. 2(f). (a) Fixed-point bifurcations of uncoupled system as function of b: PF (triangle), pitchfork at $b = 1$; SN (circle), saddle node at $b \approx 0.2984$; AH (square), Andronov-Hopf at $b \approx 0.6523$; yellow shaded region, oscillation amplitude; red dash-dotted line, $b = 1.2$. (b) MSF of coupled system with $\tau = 0.2$ and $b = 1.2$. Red triangle and circle, network eigenvalues $\gamma_1 = \gamma_2^* = i\,c$ with $c = 3.5$. (c) Time evolution of Eq. (11) started from random initial conditions close to zero for uncoupled and (d) coupled system.

D. Oscillation quenching to nonzero steady states created through coupling

Another possible scenario is one where coupling stabilizes a nonzero steady state [18,38]. For nonzero steady states x^* [with coupling function $h(x^*) \neq 0$] and coupling matrices $\mathbf{G}$ with row sum unequal zero, the coupling signal is nonvanishing, even if all oscillators are exactly on the homogeneous steady state. In this sense, the stabilization of nonzero steady states is invasive and thereby qualitatively distinct from the noninvasive stabilization of the zero steady state.

Here we discuss an example where the uncoupled systems oscillate because they are close to the Andronov-Hopf bifurcation of the zero steady state. These oscillations are quenched in the coupled system because coupling both changes the stability of the limit cycle and leads to the creation of new stable nonzero steady-state solutions. The equations we consider are

$$\dot{x}_1 = a\,x_1(t) - x_1^3(t) + b\,x_1(t-1) + c\,x_2(t-\tau), \qquad (12a)$$

$$\dot{x}_2 = a\,x_2(t) - x_2^3(t) + b\,x_2(t-1) + c\,x_1(t-\tau), \qquad (12b)$$

where $x_i, a, b, c \in \mathbb{R}$. For $a + b < 0$, the only real steady-state solution for the uncoupled systems ($c = 0$) is the zero solution ($x_1 = x_2 = 0$). In this two-oscillator case, the network eigenmode decomposition, which is the first step of the MSF approach, corresponds to a coordinate transformation to in-phase and antiphase variables. The network eigenvalue $\gamma_1 = c$ is associated with the in-phase mode $u = (x_1 + x_2)/2$ and $\gamma_2 = -c$ with the antiphase mode $v = (x_1 - x_2)/2$.

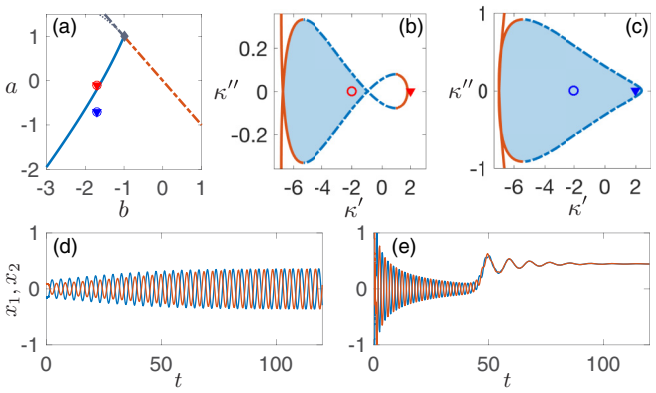

FIG. 6. Excitatory coupling with $c = 2$, $\tau = 0.33$. (a) a-b plane as in Fig. 2(f). Coupled: red triangle and circle at $a = -0.1$, $b = -1.7$ correspond to MSF in panel (b); blue triangle and circle at $a = -0.7$, $b = -1.7$ correspond to panel (c). (b) MSF for zero steady state and (c) nonzero steady state. Triangle (circle) is the in-phase (antiphase) network eigenmode. (d) Time evolution for the uncoupled and (e) coupled systems.

First consider positive coupling strengths, $c > 0$, that satisfy $a + b + c > 0$. We refer to this case as excitatory coupling. For excitatory coupling, two steady-state solutions appear on the in-phase manifold of the coupled system in addition to the zero steady state:

$$(x_1^*, x_2^*) = \pm(\sqrt{a+b+c}, \sqrt{a+b+c}), \tag{13}$$

corresponding to $u^* = \pm\sqrt{a+b+c}$, $v^* = 0$.

The uncoupled systems are unstable and close to the Andronov-Hopf bifurcation transition for the chosen parameters of $a = -0.1$ and $b = -1.7$, as is seen by the red (upper) triangle and circle in Fig. 6(a). Thus, the uncoupled systems are expected to oscillate, which is confirmed by numerical integration of Eq. (12) with $c = 0$ as shown in Fig. 6(d).

The MSF for the zero steady state is shown in Fig. 6(b). It is seen that the stable region is contained in the left complex half plane, which means that the zero steady state cannot be stabilized through direct coupling for any network topology. In particular, for the two-oscillator network with chosen coupling strength of $c = 2$, the antiphase mode is stabilized by the coupling, as is shown by the red circle in Fig. 6(b), whereas the in-phase mode has one unstable direction, as seen by the red triangle, which lies in a parameter region with unstable dimension equal to 1. This prediction is confirmed by direct numeric integration of Eq. (12), shown in Fig. 6(e), where the coupled system is initialized close to the antiphase manifold ($|u(t)| < 1 \times 10^{-5}, t \in [-1,0]$). Initially the antiphase oscillations decay and converge to $v = 0$, which is the asymptotic solution if $u = 0$. The solution starts to diverge from the zero steady state at approximately $t = 50$ because of the small yet nonzero in-phase component of the initial condition.

The linear stability of either one of the two nonzero steady-state solutions given by Eq. (13) can be determined by Eq. (8) if $a = -0.1$ is replaced by $a' = a - 3(a+b+c) = -0.7$ [the blue (lower) circle and triangle in Fig. 6(a)]. The corresponding MSF of the nonzero steady-state solution is depicted in Fig. 6(c), where it is seen that the network eigenvalues for the in-phase (blue triangle) and antiphase (blue circle) mode both fall inside the stable MSF region. In accordance with this prediction of stability, the numerical solution in Fig. 6(e) approaches the nonzero homogeneous steady state, $x_1^* = x_2^* \approx 0.45$.

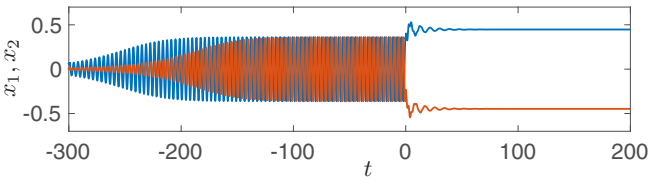

FIG. 7. Inhibitory coupling with $a = -0.1$, $b = -1.7$, $c = -2$, $\tau = 0.33$: $t < 0$ uncoupled, $t > 0$ coupled.

In this example, oscillations are quenched to a homogeneous steady state; therefore, this is again a form of amplitude death. The difference to amplitude death in the strict sense is that the stable nonzero homogeneous steady state is created through the coupling. It does not exist for the uncoupled systems. Furthermore, the zero steady state remains unstable after coupling.

One may also consider inhibitory coupling, which corresponds to negative coupling strengths, $c < 0$. One finds that replacing c by $-c$ is equivalent to an exchange of in-phase and antiphase variables. Thus, coupling with $c = -2$ results in oscillation quenching and the creation of two stable inhomogeneous nonzero steady states

$$(x_1^*, x_2^*) = \pm(\sqrt{a+b-c}, -\sqrt{a+b-c}), \tag{14}$$

or, equivalently, $u^* = 0, v^* = \pm\sqrt{a+b-c}$. The results of numerical integration shown in Fig. 7 confirm this prediction. The initially uncoupled systems ($t < 0$) each converge to a limit cycle, whereas the coupled systems with inhibitory links ($t > 0$) quickly converge to an inhomogeneous steady state, where the two systems have nonzero constant values of opposite sign. That is, oscillations are quenched to an inhomogeneous steady state, an example of oscillation death.

V. AMPLITUDE DEATH OF DIRECTLY COUPLED SECOND-ORDER DELAY DIFFERENTIAL EQUATIONS

We have shown that amplitude death in the strict sense is not possible for directly coupled networks of identical first-order DDEs. It becomes a possibility if the complexity of the node dynamics is increased and second-order DDEs are considered, as we demonstrate on the example of a model that describes two coupled optoelectronic feedback oscillators [24–27]:

$$\dot{\mathbf{x}}_j(t) = \mathbf{A}\mathbf{x}_j(t) + g_{\mathrm{sf}}\,\mathbf{b}\,f(u^{\tau_{\mathrm{sf}}}) + \sum_{\ell \neq j} g_{j\ell}\mathbf{b}\,f(u^{\tau_c}), \tag{15}$$

where $j = 1,2$ labels the oscillator, $\mathbf{x}_j = (u_j, v_j)^T \in \mathbb{R}^2$, $u^\tau = u(t-\tau)$, τ_{sf} is the self-feedback delay within each node, τ_c the coupling delay, $\mathbf{b} = (1,0)^T$, and

$$\mathbf{A} = \begin{pmatrix} -1 & -1 \\ \left[2\pi\, T_0^{-1}\right]^2 & 0 \end{pmatrix}. \tag{16}$$

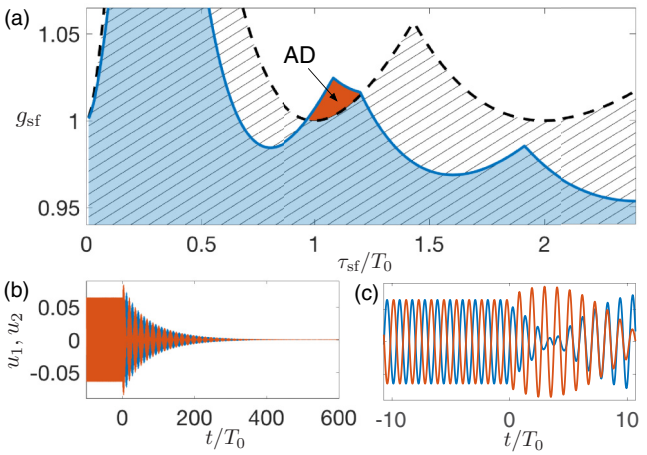

FIG. 8. Second-order DDE, Eq. (15): (a) Region of stable steady state for uncoupled [hatched, below the thick dashed (black) line] and directly coupled [shaded, below the thick solid (blue) line] system. AD: amplitude death region [dark (red) shade]. (b) Time evolution of $u(t)$ with coupling turned on at $t = 0$. (c) Zoom for t close to $t = 0$. (Initial conditions: $|u| < 0.001$, transient not shown). Parameters used: $T_0 = 11.47$, $d = 1.71$, $g_{sf} = 1.01$ $\tau_c = 0.124$, $\tau_{sf} = 12.435$. This implies ratios $\tau_c/\tau_{sf} \approx 0.01$ and $\tau_{sf}/T_0 \approx 1.08$.

The node nonlinearity and coupling function are identical, given by $f[x] = \sin(2d\ \tanh[x])/(2d)$, and describe the transfer characteristic of a Mach-Zehnder modulator at maximum linear feedback gain, where d is a fixed parameter and the tanh function models saturation of the drive electronics [27]. Oscillations in an optoelectronic device, i.e., a network node, arise due to this nonlinearity and self-feedback of the signal $u(t)$ that is delayed by τ_{sf}, amplified by a factor g_{sf}, and bandpass filtered. Physically, u represents the detector voltage corresponding to the measured optical power. The parameter T_0^{-1} represents the dimensionless frequency of maximum transmission of the bandpass filter.

The zero steady state of the uncoupled oscillators loses stability through supercritical Andronov-Hopf bifurcations [26,39]. The stability region of each uncoupled oscillator as a function of the delay τ_{sf} and gain g_{sf} is shown as a black hatched region in Fig. 8(a). It is seen that the positive feedback gain necessary to destabilize the steady state is minimized at self-feedback delays that are integer multiples of T_0, where the Andronov-Hopf bifurcation occurs at $g_{sf}^{AH} = 1$.

Depicted as the blue shaded region in Fig. 8(a) is the steady-state stability region of two optoelectronic oscillators that interact via unequal-sign direct coupling links of weight $g_{12} = -g_{21} = 0.25$ and coupling delays satisfying $\tau_c/\tau_{sf} = 0.01$. It is seen that there exists an amplitude death region for parameters τ_{sf} and gain g_{sf} close to the stability minimum. The result of direct numerical integration [see Fig. 8(b)] confirms that coupling destroys limit cycle oscillations and stabilizes the zero steady state.

We find that the amplitude death region disappears in the weak-coupling limit ($|g_{j\ell}| < |g_{sf} - g_{sf}^{AH}|$) and in the large delay limit ($\tau_c/\tau_{sf} \gg 1$) in agreement with Ref. [30] and Sec. II, respectively. In other words, amplitude death in the strict sense is possible in directly coupled networks of second-order DDEs but the coupling strength has to be sufficiently strong and the coupling delay has to be short compared to internal time scales.

VI. CONCLUSIONS

In this paper we show that changing the type of coupling function from diffusive to direct coupling leads to qualitative differences in the emergence of amplitude death, a phenomenon where systems that exhibit self-sustained oscillatory behavior when uncoupled cease to oscillate when linked together in a network. We show, for example, that direct coupling makes amplitude death impossible for delay coupled identical Stuart-Landau oscillators. Although amplitude death is less likely in directly coupled networks as compared to diffusively coupled networks, we find that amplitude death may occur if the node dynamics are sufficiently complex, coupling is sufficiently strong, and the coupling delay is short compared to internal time scales.

A main contribution of this paper is the rigorous treatment of directly coupled networks with identical coupling delays that have node dynamics governed by ODEs and by first-order DDEs. Since time delay is ubiquitous in coupled systems and since inputs to realistic systems are often in the form of direct injection of signals, our work provides an important basis to understand and control oscillation quenching in biological, chemical, photonics, and electronic systems.

One motivation for investigating direct coupling stems from experimental implementations of optoelectronic oscillators [24–27]. The analysis of the corresponding delay-coupled second-order DDE shows that amplitude death in the strict sense is possible but only if the parameters of the individual oscillators are chosen from a very small parameter region (see Fig. 8). In this context it is of practical interest to study the robustness of the amplitude death state under external noise and small mismatches of both the node parameters and the coupling delays.

ACKNOWLEDGMENTS

The author thanks Eckehard Schöll's group at the TU Berlin for their hospitality and acknowledges Eckehard Schöll, Judith Lehnert, and Chiranjit Mitra for valuable discussions. This work was supported by a faculty research visit grant of the Deutscher Akademischer Austauschdienst (DAAD).

APPENDIX A: STEADY-STATE STABILITY OF LINEAR FIRST-ORDER DDEs WITH COMPLEX COEFFICIENTS

Here we study the stability of the zero steady state of $\dot{z} = \alpha\, z(t) + \beta\, z(t-1)$ for general complex coefficients α and β by considering the characteristic equation

$$\Lambda = \alpha + \beta\, e^{-\Lambda}. \tag{A1}$$

We note that, on rescaling time by τ, Eq. (6) maps onto Eq. (A1) with $\alpha = a\,\tau + i\,\omega_0\,\tau$ and $\beta = \kappa\, r\, \tau\, e^{i\phi_0}$. The countably infinite number of roots of Eq. (A1) can be written in terms of the branches k of the Lambert W function [40] as

$$\Lambda_k = \alpha + \mathrm{W}_k(\beta e^{-\alpha}). \tag{A2}$$

The principal branch $W_0(\cdot)$ has the largest real part of all branches for any given complex argument. Thus, the steady state is stable if

$$\Lambda_0' = \alpha' + \mathrm{Re}W_0(|\beta|e^{-\alpha'}e^{i\phi}) < 0, \tag{A3}$$

where we denote the real and imaginary parts of Λ_k as $\Lambda_k = \Lambda_k' + i\,\Lambda_k''$ and α as $\alpha = \alpha' + i\,\alpha''$. The phase ϕ is defined as $\phi = \arg\beta - \alpha''$.

The problem is therefore reduced to one of three real-valued relevant parameters α',$|\beta|$, and ϕ. It is visually appealing to plot the stability region in the 3D space formed by α',$\mathrm{Re}(\zeta)$, and $\mathrm{Im}(\zeta)$, where $\zeta = |\beta|e^{-\alpha'}e^{i\phi}$ [see Fig. 1(a)].

It will turn out to be convenient to consider the minimum of Λ_0' with respect to the phase ϕ, while the parameters α' and $|\beta|$ are assumed to be held fixed. The first derivative of Λ_0' with respect to ϕ gives

$$\frac{\partial\Lambda_0'}{\partial\phi} = \frac{\mathrm{Im}\,W_0(\zeta)}{|1+W_0(\zeta)|^2}. \tag{A4}$$

The derivative is zero and Λ_0' is an extremum if the imaginary part of the principal branch W_0 of the Lambert W function is zero, which is true if and only if its argument ζ is real valued and in the interval $[-e^{-1},\infty)$. The argument is real valued and positive if $\phi = 0$. The argument is real valued and negative if $\phi = \pi$. The second derivative of Λ_0' evaluated at the extremum, where $\mathrm{Im}W_0(\zeta) = 0$, is

$$\frac{\partial^2\Lambda_0'}{\partial\phi^2} = -\frac{\mathrm{Re}W_0(\zeta)}{[1+\mathrm{Re}W_0(\zeta)]^3}, \tag{A5}$$

which is positive if $\zeta \in (-e^{-1},0)$, i.e., if $\phi = \pi$, and negative if $\zeta \in (0,\infty)$, i.e., if $\phi = 0$. Therefore, the real part of the maximal root is minimized if $\phi = \pi$,

$$\Lambda_0'|_{\text{optimal }\phi} = \alpha' + \mathrm{Re}W_0(-|\beta|e^{-\alpha'}). \tag{A6}$$

Recalling that the minimal real part of the principal branch of the Lambert W function is given by $\min_{|z|}\mathrm{Re}[W_0(-|z|)] = W_0(-e^{-1}) = -1$, we find that the optimal choice of $|\beta|$ is $|\beta| = e^{\alpha'-1}$, implying

$$\Lambda_{0,\mathrm{opt}}' = \alpha' - 1. \tag{A7}$$

This shows that for any choice of $|\beta| \in (0,\infty)$ and $\phi \in (-\pi,\pi]$ there exists at least one characteristic value Λ with positive real part, if $\alpha' > 1$.

The boundary of the steady-state stability region can be found analytically. For all fixed $\alpha' < 1$, it is given by the solution of $\Lambda_0' = 0$ as a function of $|\beta|$ and ϕ, i.e., one considers $|\beta|$ to be a free parameter. Using the definition of the Lambert W function, $W(z)\exp[W(z)] = z$, in Eq. (A2) with $k = 0$ to obtain an equation free of W_0 and subsequently eliminating the imaginary part Λ_0'', we find

$$\phi^{\pm}(|\beta|) = \pm\left[\arccos\left(-\frac{\alpha'}{|\beta|}\right) + \sqrt{|\beta|^2-\alpha'^2}\right], \tag{A8}$$

where $|\beta| \in (\alpha',|\beta|_{\max})$ and $|\beta|_{\max}$ is implicitly determined as the solution of $\phi^+(|\beta|_{\max}) = \pi$. The boundary given by Eq. (A8) corresponds to the red line in Fig. 1(b).

For the existence of a stable steady state of directly coupled networks, it is important to consider the stability region defined by $\Lambda_0' < 0$ with the additional assumption that $\mathrm{Re}(\zeta) = 0$. We find that the boundary as a function of α' and $\mathrm{Im}(\zeta)$ is given in parametric form by $\mathrm{Im}(\zeta) = \Omega/\cos(\Omega)$, $\alpha' = -\Omega\tan(\Omega)$ $(-\pi/2 < \Omega < \pi/2)$. This boundary corresponds to the yellow line in Fig. 1(d). It is seen that for directly coupled networks stable steady states cannot exist for $\alpha' > 0$.

APPENDIX B: THE ZERO COUPLING-DELAY LIMIT

We consider the zero coupling-delay limit in directly coupled networks of first-order DDEs with linear dynamics modeled by Eq. (7). For $\tau = 0$, the characteristic equation, Eq. (8), is identical to Eq. (A1) if the coefficients are chosen as $\alpha = a + \kappa' + i\kappa''$ and $\beta = b$. Utilizing the results of Appendix A, one finds that the real part of the maximum root is given by $\Lambda_0' = \alpha' + \mathrm{Re}\,W_0(\zeta)$, where

$$\zeta = \begin{cases} |b|\,e^{-(a+\kappa')}\,e^{i(\pi-\kappa'')} & b \leqslant 0 \\ |b|\,e^{-(a+\kappa')}\,e^{-i\,\kappa''} & b > 0. \end{cases} \tag{B1}$$

Our goal is to determine the region in the a-b parameter plane for which there exist networks with a stable steady state. This is done within the MSF approach by determining the root with maximum real part Λ_0' for the optimal choice of κ. We argued that $\kappa' = 0$ is optimal. One notes that $\phi = \pi - \kappa''$ if $b \leqslant 0$ and $\phi = -\kappa''$ if $b > 0$, as seen by comparing Eq. (B1) and Eq. (A3). One finds that the real part of the maximum root is minimized if $\phi = \pi$, by the same arguments as in Appendix A. Together, this yields the following minimized maximum root

$$\Lambda_0'|_{\mathrm{opt}} = \begin{cases} a + \mathrm{Re}\,W_0(b\,e^{-a}) & b \leqslant 0\ (\kappa'' = 0) \\ a + \mathrm{Re}\,W_0(-b\,e^{-a}) & b > 0\ (\kappa'' = \pi). \end{cases} \tag{B2}$$

The $b \leqslant 0$ case is identical to the stability of a single uncoupled first-order DDE, i.e., characteristic equation Eq. (8) with $\kappa = 0$. The same is true for the $b > 0$ case, if b in Eq. (8) is replaced by $-b$. In other words, the region of steady-state stability for optimal κ consists of the stability region of a single uncoupled first-order DDE for negative b and its mirror image for positive b. This stability region is shown in Fig. 4(b) as the shaded area below the red line. This means that, in addition to the parameter region where the uncoupled nodes are already stable [blue (dark gray) region in Fig. 4(b)], there exists a parameter region where direct coupling can stabilize the zero-steady state [green (light gray) region in Fig. 4(b)] if the network topology and coupling strengths are chosen optimally.

[1] Y. Kuramoto, *Chemical Oscillations, Waves, and Turbulence* (Springer, Berlin, 1984).

[2] L. Illing, D. J. Gauthier, and R. Roy, in *Advances in Atomic, Molecular, and Optical Physics*, edited by P. R. Berman, E.

Arimondo, and C. Lin (Elsevier, Amsterdam, 2007), Vol. 54, pp. 615.
[3] K. Lüdge (ed.), *Nonlinear Laser Dynamics—From Quantum Dots to Cryptography* (Wiley-VCH, Weinheim, 2012).
[4] E. M. Izhikevich, *Dynamical Systems in Neuroscience: The Geometry of Excitability and Bursting* (MIT Press, Cambridge, 2007).
[5] J. D. Murray, *Mathematical Biology* (Springer Verlag, New York, 2002), 3rd ed.
[6] J. Stricker, S. Cookson, M. R. Bennett, W. H. Mather, L. S. Tsimring, and J. Hasty, Nature **456**, 516 (2008).
[7] M. R. Tinsley, S. Nkomo, and K. Showalter, Nat. Phys. **8**, 662 (2012).
[8] C. R. S. Williams, T. E. Murphy, R. Roy, F. Sorrentino, T. Dahms, and E. Schöll, Phys. Rev. Lett. **110**, 064104 (2013).
[9] L. M. Pecora, F. Sorrentino, A. M. Hagerstrom, T. E. Murphy, and R. Roy, Nat. Commun. **5**, 4079 (2014).
[10] D. G. Aronson, G. B. Ermentrout, and N. Kopell, Physica D **41**, 403 (1990).
[11] R. E. Mirollo and S. H. Strogatz, J. Stat. Phys. **60**, 245 (1990).
[12] E. Schöll and H. G. Schuster (eds.), *Handbook on Chaos Control* (Wiley-VCH, Weinheim, 2008), 2nd ed.
[13] P. J. Uhlhaas and W. Singer, Neuron **52**, 155 (2006).
[14] A. Prasad, M. Dhamala, B. M. Adhikari, and R. Ramaswamy, Phys. Rev. E **81**, 027201 (2010).
[15] A. Koseska, E. Volkov, and J. Kurths, Phys. Rep. **531**, 173 (2013).
[16] R. Karnatak, R. Ramaswamy, and A. Prasad, Phys. Rev. E **76**, 035201 (2007).
[17] D. V. Ramana Reddy, A. Sen, and G. L. Johnston, Phys. Rev. Lett. **80**, 5109 (1998).
[18] G. Saxena, A. Prasad, and R. Ramaswamy, Phys. Rep. **521**, 205 (2012).
[19] O. D'Huys, R. Vicente, J. Danckaert, and I. Fischer, Chaos **20**, 043127 (2010).
[20] J. M. Höfener, G. C. Sethia, and T. Gross, Philos. Trans. R. Soc. A **371**, 20120462 (2013).
[21] C.-U. Choe, T. Dahms, P. Hövel, and E. Schöll, Phys. Rev. E **81**, 025205 (2010).
[22] A. Selivanov, J. Lehnert, A. Fradkov, and E. Schöll, Phys. Rev. E **91**, 012906 (2015).
[23] A. Argyris, D. Syvridis, L. Larger, V. Annovazzi-Lodi, P. Colet, I. Fischer, J. Garcia-Ojalvo, C. R. Mirasso, L. Pesquera, and K. A. Shore, Nature **438**, 343 (2005).
[24] M. Peil, M. Jacquot, Y. K. Chembo, L. Larger, and T. Erneux, Phys. Rev. E **79**, 026208 (2009).
[25] K. E. Callan, L. Illing, Z. Gao, D. J. Gauthier, and E. Schöll, Phys. Rev. Lett. **104**, 113901 (2010).
[26] L. Illing, G. Hoth, L. Shareshian, and C. May, Phys. Rev. E **83**, 026107 (2011).
[27] L. Illing, C. D. Panda, and L. Shareshian, Phys. Rev. E **84**, 016213 (2011).
[28] M.-Y. Kim, R. Roy, J. L. Aron, T. W. Carr, and I. B. Schwartz, Phys. Rev. Lett. **94**, 088101 (2005).
[29] A. Gjurchinovski, A. Zakharova, and E. Schöll, Phys. Rev. E **89**, 032915 (2014).
[30] F. M. Atay, *Complex Time-Delay Systems* (Springer-Verlag, Berlin, 2010), p. 45.
[31] M. Lichtner, M. Wolfrum, and S. Yanchuk, SIAM J. Math. Anal. **43**, 788 (2011).
[32] A. Zakharova, I. Schneider, Y. N. Kyrychko, K. B. Blyuss, A. Koseska, B. Fiedler, and E. Schöll, Europhys. Lett. **104**, 50004 (2013).
[33] L. M. Pecora and T. L. Carroll, Phys. Rev. Lett. **80**, 2109 (1998).
[34] The two-oscillator system with unequal coupling delay $\dot{\mathbf{x}}_1 = \mathbf{g}[\mathbf{x}_1(t),\mathbf{x}_2(t-\tau_{12})], \dot{\mathbf{x}}_2 = \mathbf{f}[\mathbf{x}_2(t),\mathbf{x}_1(t-\tau_{21})]$ is mapped under coordinate change $\bar{\mathbf{x}}_1(t) = \mathbf{x}_1(t)$ and $\bar{\mathbf{x}}_2(t) = \mathbf{x}_2(t+\Delta)$, where $\Delta = (\tau_{21}-\tau_{12})/2$, to $\dot{\bar{\mathbf{x}}}_1 = \mathbf{g}[\bar{\mathbf{x}}_1(t),\bar{\mathbf{x}}_2(t-\tau)], \dot{\bar{\mathbf{x}}}_2 = \mathbf{f}[\bar{\mathbf{x}}_2(t),\bar{\mathbf{x}}_1(t-\tau)]$, where $\tau = (\tau_{21}+\tau_{12})/2$.
[35] B. F. Redmond, V. G. LeBlanc, and A. Longtin, Physica D **166**, 131 (2002).
[36] T. Erneux, *Applied Delay Differential Equations of Surveys and Tutorials in the Applied Mathematical Sciences* (Springer, Berlin, 2009), Vol. 3.
[37] L. Larger, J. P. Goedgebuer, and T. Erneux, Phys. Rev. E **69**, 036210 (2004).
[38] C. Mitra, G. Ambika, and S. Banerjee, Chaos Solitons Fract. **69**, 188 (2014).
[39] L. Illing and D. J. Gauthier, Physica D **210**, 180 (2005).
[40] R. M. Corless, G. H. Gonnet, D. E. G. Hare, D. J. Jeffrey, and D. E. Knuth, Adv. Comput. Math. **5**, 329 (1996).